Available online at www.sciencedirect.com
SCIENCE DIRECT®
Journal of Magnetic Resonance 178 (2006) 77–87
JMR Journal of Magnetic Resonance
www.elsevier.com/locate/jmr

Rectifying system-specific errors in NMR relaxation measurements

Norma H. Pawley, M. Daniel Clark, Ryszard Michalczyk *

Bioscience Division, B-3, MS G758, Los Alamos National Laboratory, Los Alamos, NM 87545, USA

Received 19 May 2005; revised 11 August 2005
Available online 4 October 2005

Abstract

^{15}N spin relaxation parameters provide a powerful tool for probing the internal dynamics and thermodynamics of proteins. The biological insight provided by these experiments often involves interpretation of small changes in relaxation parameters. This, in turn, requires careful data analysis, especially in the identification and treatment of systematic error. While progress continues on reduction of experiment-specific errors associated with pulse sequences, system-specific sources of error have received far less attention. The impact of these errors varies between facilities, spectrometers, and biological samples. We demonstrate that performing a series of control experiments along with relaxation measurements can help identify, quantify, and isolate sources of system-specific error, and, in some cases, correct for systematic changes. We further demonstrate that control experiments can be performed without significant loss of spectrometer time, and lead to more accurate relaxation parameter values.

Keywords: NMR; Relaxation dispersion; Protein dynamics; Systematic error

1. Introduction

^{15}N spin relaxation parameters provide a powerful tool for probing the internal dynamics and thermodynamics of proteins. They have been used to gain insight on protein folding [1], catalysis [2], and ligand binding [3], as well as conformational entropy and activation energies [4–6]. These biological insights often involve interpretation of small changes in relaxation parameters and require careful data analysis.

Careful data analysis requires cautious treatment of both random and systematic errors. A typical protocol for estimation of random errors includes measurement of duplicates or replicates [7,8], and setting of a minimum error (such as standard deviation of baseplane noise [9], or an ad hoc value, such as 2% [10,11]). Treatment of systematic errors is more complicated. Over the years, a number of sources of systematic error have been identified, and their impact on relaxation analysis mitigated. Examples of experiment-specific sources of error that have been addressed include scalar coupling [12], cross-relaxation and dipolar/CSA cross-correlation [12], off-resonance effects [13–16], sample heating [17], and decoupling effects [18]. Examples of system-specific sources of error that have been addressed include magnetic field inhomogeneity [19] and peak intensity analysis [20]. While progress continues on identification and elimination of experiment-specific sources of error, system-specific sources of error have received far less attention. The impact of these errors varies between facilities, spectrometers, and biological samples.

1.1. Historical treatments of systematic error were sufficient for historical measurements

Systematic changes in peak intensity over a series of relaxation measurements have long been observed and reported [8]. One of the most common ways to address these systematic changes is to fold them into the random error by sampling points along the decay curve in ''pseudo-random'' order, rather than sequentially in time. The impact of this ''random'' error is then reduced by sampling the intensity at a large number of time points along the decay curve with repeated measurements at individual time

* Corresponding author. Fax: +1 505 667 0110.
E-mail address: rmichalczyk@lanl.gov (R. Michalczyk).

1090-7807/$ - see front matter © 2005 Elsevier Inc. All rights reserved.
doi:10.1016/j.jmr.2005.08.017

points [21,22]. This method has been sufficient for analysis of exponential decay functions, $I(t) = e^{-Rt}$. When measured over an appropriate range of time points, the amplitude of an exponential decay is much larger than the size of typical systematic and random errors. Small systematic errors have only a slight effect on the accurate extraction of R. For example, systematic errors in intensity of up to 5% in measurements of R_2 at 500 MHz cause deviations of only 0.4–1.3% in the extracted value of R_2, depending on the form of the underlying error function and the order in which data are acquired (vide infra). Hence, while various forms of systematic error can change the percent accuracy of extracted R_2 values by more than a factor of three, the least accurate value is still within 1.3% of the "true" value, suggesting that historical treatments of systematic error were sufficient for exponential decay measurements.

1.2. The effects of systematic error can be mitigated by transferring changes in intensity to changes in line shape

More recently, Orekhov et al. [23] have proposed that relaxation measurements be performed in an "interleaved manner." This approach transfers systematic error from the time domain into the frequency domain, and trades systematic changes in intensity, $I(t)$, for systematic changes in line-shape, $I(\omega_N)$. This method can be very effective in reducing the impact of systematic error. Employing this method requires implementation of four changes: (1) adapting the relaxation experiments to increment the relaxation delay for each ω_N before incrementing ω_N (trivial for Varian BioPack users); (2) separating the arrayed fids for data processing; (3) shifting from analysis of peak volumes to analysis of peak intensities; and (4) verifying that extracted values of chemical exchange are not correlated with ω_N (a phenomenon that may be observed if the relaxation rate changes as a function of time). Unfortunately, this method has not been widely adopted—a cited reference search reveals citations of this method by only four other groups.

1.3. New measurements require new treatments of systematic error

In recent years, relaxation dispersion measurements have been increasing in popularity, largely displacing traditional measurements of R_2 at a single ν_{CPMG} frequency. These dispersion curves can be difficult to characterize at low spectrometer frequencies (500–600 MHz), due to shallow curvature and large experimental error [24–26]. For example, at 500 MHz, systematic errors in intensity of up to 5% can cause deviations in the extracted value of $R_2(\nu_{CPMG} = \infty)$ that range from 1.3 to 36%, depending on the form of the underlying error function and the order in which data are acquired (vide infra). At higher spectrometer frequencies, dispersion curves are more easily characterized: at 800 MHz, systematic errors in intensity of up to 5% cause deviations of less than 1% in the extracted value of $R_2(\nu_{CPMG} = \infty)$ (vide infra). However, the extraction of meaningful exchange parameters from relaxation data requires knowledge of the exchange timescale [25], and hence, characterization of dispersion curves at multiple field strengths [24,27,28]. It is necessary, therefore, to reduce experimental errors sufficiently that dispersion curves can be characterized at low field strengths, as well.

We demonstrate that performing a series of control experiments along with relaxation measurements can help identify and isolate sources of systematic error, and, in some cases, correct for systematic changes in the state of the system. We further demonstrate that the benefits of control experiments can be gained without significant loss of spectrometer time and without alteration of pulse sequences or data processing protocols.

2. Results and discussion

2.1. Effect of systematic error and data acquisition order on extracted relaxation parameters

As noted in Section 1, three main factors determine the impact of systematic errors on the accuracy and precision of extracted relaxation rates: the shape of the curve, the underlying form of the error, and the order in which data points are collected. To evaluate the impact of systematic error on extracted relaxation rates we examined two types of curves, exponential decay and relaxation dispersion. For each curve we explored five different cases, sampling from two types of underlying systematic error (systematic increase or systematic decrease in intensity), and four possible collection orders (increasing increment, decreasing increment, alternating large and small increments [triangular], and "pseudo-random," see Supplemental Figs. S1 and S2). Models were constructed as described in Sections 4.6 and 4.7.

For the exponential decay curve, changes in the error function and collection order caused changes of more than a factor of three in the percent error of the fitted parameters; however, all extracted relaxation rates were within an acceptable range of accuracy (errors of 0.4–1.3%, see Supplemental Table S1A). In contrast, for the relaxation dispersion curve simulated at 500 MHz, changes in the error function and data collection order produced changes of more than an order of magnitude in the percent error of the fitted parameters, with errors in $R_2(\nu_{CPMG} = \infty)$ ranging from 1.3 to 36% and errors in τ_{ex} ranging from 13 to 94% (details in Supplemental Table S1B).

For the two curves and five cases we considered, the most accurate values of R_2 and $R_2(\nu_{CPMG} = \infty)$ were obtained for a systematic decrease in intensity with data points measured in order of decreasing increment (Supplemental Figs. S1a and S2a). The least accurate values of R_2 and $R_2(\nu_{CPMG} = \infty)$ were obtained for a systematic increase in intensity and points measured in order of alternating increment (triangular function, Supplemental Figs. S1b and S2b—notably, this function also provides insight into the

potential impact of non-linear systematic error with points measured in order of increasing or decreasing increment).

Three important points can be drawn from these simulations. First, the cases that yield the most accurate parameters do not correspond to the best fit based on reduced χ^2 values—a reminder that quality of fit criteria can not be used as a substitute for error estimates in the presence of systematic error. Second, the most accurate parameter values were *not* obtained by acquiring data points in "pseudo-random" order. Third, for relaxation dispersion curves, knowledge of the form of the underlying error is critical, since the form of the error function and the data collection order strongly affect the accuracy of extracted parameters, and may compromise data interpretation.

2.2. System-specific systematic error can be identified and quantified using control experiments

Tuning, shim quality, sample quality (aggregation/degradation), room temperature, atmospheric pressure, and vibration levels can vary on a time scale of minutes to days and cause systematic changes in peak intensities and volumes across a series of NMR experiments. However, these systematic changes can be difficult to observe and quantify without prior knowledge of the "true" form of the function governing the volumes, as illustrated by the simulated relaxation dispersion curves shown in Figs. 1A and B (details in Section 4). Simulated values of $R_{2,\mathrm{eff}}(\nu_{\mathrm{CPMG}})$ in the presence up to 5% systematic error in peak intensity (systematic decrease in intensity, applied in order of increasing increment) are shown in Fig. 1A. The points can be fit very well using the fast-exchange equation, yielding the values: $R_{2,\mathrm{eff}}(\nu_{\mathrm{CPMG}}=\infty)=18.7\ \mathrm{s}^{-1}$, $p_a \times p_b \times \delta\omega^2 = 7.5\times10^3\ \mathrm{s}^{-2}$, $\tau_{ex}=5.0\times10^{-4}$ s, reduced chi-square $(\chi^2_\nu)\sim 1$. The inaccuracy of the fit can only be observed by comparing the values obtained in the presence of systematic error with the "true" values of $R_{2,\mathrm{eff}}(\nu_{\mathrm{CPMG}})$, in the absence of systematic error, as shown in Fig. 1B: $R_{2,\mathrm{eff}}(\nu_{\mathrm{CPMG}}=\infty)=20.0\ \mathrm{s}^{-1}$, $p_a \times p_b \times \delta\omega^2 = 3.2\times10^3\ \mathrm{s}^{-2}$, $\tau_{ex}=9.3\times10^{-4}$ s. Although the data in Fig. 1A were well fit, the fit was not accurate. The percent error in the parameters corresponds to 6.6, 140, and 46%, respectively.

To observe systematic changes in the state of a system and draw conclusions regarding the accuracy of a measurement, the "true" form of the function governing the measurement must be known a priori. One way to accomplish this is to perform control experiments along with data collection [29]. The advantage of control experiments is that the "correct" functional form is known: peak volumes should remain constant across a series of experiments. If the peak volumes are normalized by their values in the first measured experiment then the constant should equal 1. This knowledge of the expected functional form allows deviations to be readily observed and quantified, as illustrated by the series of control measurements shown in Fig. 1C. Through statistical analysis one can assess the probability that the observed deviations are attributable to random error alone, or whether systematic error is likely to be present. For example, for the data shown in Fig. 1C the probability of obtaining the observed deviations from the expected constant value of 1 under the influence of only random error is less than 3×10^{-23} (details in Section 4.4).

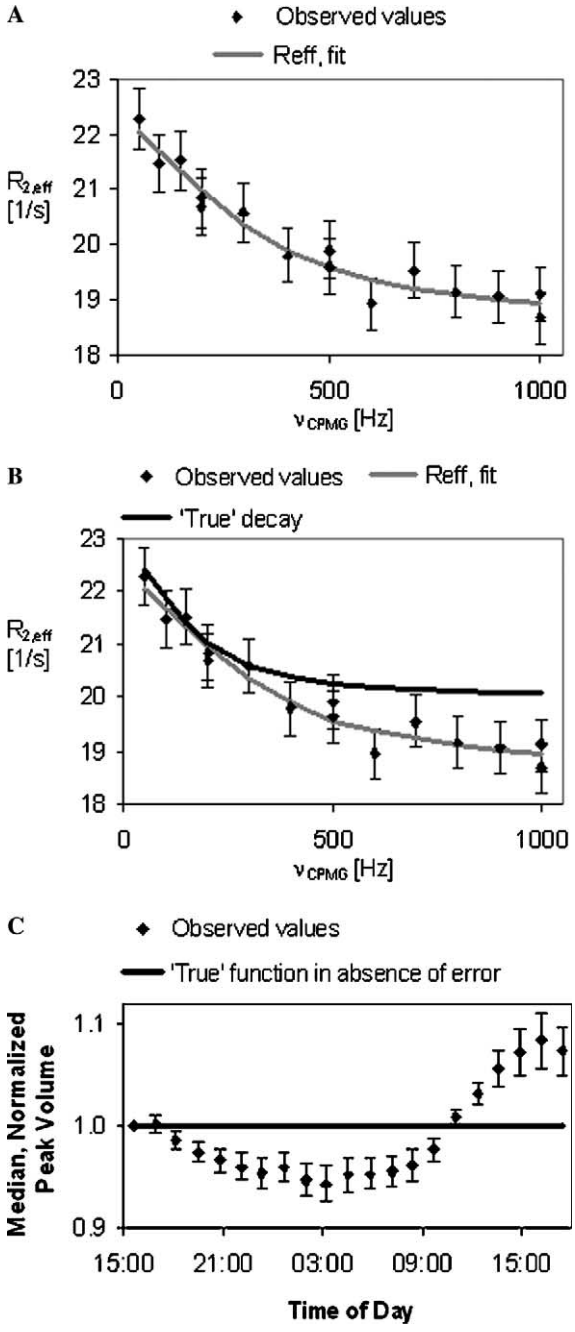

Fig. 1. Systematic changes can be difficult to observe or quantify without prior knowledge of the "true" form of the function governing the volumes. (A) Simulated values of $R_{2,\mathrm{eff}}(\nu_{\mathrm{CPMG}})$ in the presence of up to 5% systematic error in peak intensity. (B) Comparison of "true" values of $R_{2,\mathrm{eff}}(\nu_{\mathrm{CPMG}})$ in the absence of systematic error with the fit obtained in the presence of systematic error. (C) Control experiments showing systematic deviations from the expected constant value as a function of time. Error bars represent the standard deviation of peak volumes across the protein.

2.3. Choosing a control experiment for identification of systematic changes

Any experiment collected independently of the desired data, and repeated identically over the entire measurement period can be used to identify systematic changes. The choice of control experiment is guided primarily by the amount of information desired, and the amount of time available. We have explored a number of possible control experiments, described in detail in Section 4.2. The test controls included measuring the lock level, measuring the water signal intensity (simple one-pulse experiment), measuring the integral of the 1D proton spectrum of the protein (Watergate experiment), measuring shorter versions of the experiment being used for data collection, and measuring the same experiment being used for data collection. Each of these controls has been shown to correlate with changes in the state of the system and changes in the desired data; however, the degree of correlation and the information content of these controls vary. Of the fast experiments (lock level, water intensity, and 1D proton spectrum), the best correlation was obtained by observing changes in the water signal intensity. Measurements of water signal intensity are valuable for monitoring the state of the system and detecting systematic effects that are not sample related. Lengthier experiments with greater information content, such as 2D protein spectra, are necessary if one suspects systematic effects that impact the protein without impacting the solution (such as sample degradation), or if one wishes to go beyond detection, to remediation, as described in detail below.

2.4. Mining information from control experiments

A single series of control measurements can be mined for a variety of analyses. In addition to the size of the systematic error, control experiments reveal a number of important features of the error. For example, the volumes shown in Fig. 1C recover after the initial loss. This demonstrates that the dominant systematic effect observed in these controls does not arise from an irreversible process such as protein degradation. Opposite trends are observed during morning and evening rush hours, suggesting that the dominant effect is not vibration. The changes appear to reflect a day/night cycle, which is suggestive of temperature and/or pressure effects. Following the observation of systematic trends, external measurement devices such as temperature sensors, vibration sensors, or oscilloscopes can be used to further isolate root causes, demonstrate correlations, and establish whether the source of systematic error is continuous or intermittent.

Control experiments reveal that the standard deviation of peak volumes obtained in a single experiment also varies as a function of time (Fig. 1C), suggesting that a limited number of replicates will not necessarily provide a general estimate of error. (For example, the five smallest deviations [points 2–4, 15–16] have an average size of less than 0.01, while the five largest deviations [points 10, 18–21] have an average size greater than 0.02.) Changes in peak volume reproducibility as a function of time have been observed previously [8], although the physical source of the change was not identified.

2.5. An example of system-specific systematic error detected using control experiments

A set of control experiments (details in Section 4.1) measured under varied room temperature conditions shows a surprisingly large contribution to systematic error from room temperature instability. Systematic volume changes as a function of room temperature at constant sample temperature are shown in Fig. 2. It might be expected that a room temperature change of more than 7 °F (Fig. 2A) would negatively impact measurement reproducibility, due to factors such as changes in probe tuning and variations in other electronic components of the system. However, the finding that a room temperature change of less than ±1 °F is sufficient to introduce a systematic deviation of up to 3.5% in control experiments (Figs. 2B and C), was unexpected. A room temperature change of less than ±2 °F can increase the systematic deviation to 6.6% (Fig. 2C). It is worth noting that these two points (±2 and ±1 °F) are within the recommended temperature range of the Bruker AVANCE Site Planning Guide for 500 MHz and higher field spectrometers, respectively. This suggests that other facilities, operating within the manufacturer's specifications, may experience systematic changes in peak volumes similar to those reported here. Systematic changes resulting from temperature fluctuations may not be revealed by re-measuring a relaxation data set, unless the experiments are collected in a different order, or the time-dependence of the error changes.

2.6. System-specific systematic error can be reduced using control experiments: proof of principle

We hypothesized that when changes in peak volumes are correlated and continuous (an assumption that is expected to be true for most of the sources of error listed above, with the exception of vibration), peak volumes from a given experiment could be re-normalized using the average volume of the same peak observed in the immediately preceding and following control experiments (see Section 4.5). To show that this hypothesis is correct, we demonstrate that a set of control experiments for which the systematic changes are correlated and continuous is self-correcting.

Normalized peak volumes from a set of control measurements are shown in Fig. 3A. The values differ significantly from the constant value of 1—the expected functional form in the absence of error. The same data, following re-normalization, are shown in Fig. 3B. The re-normalization successfully reduces the deviations from the expected functional form, as shown in Figs. 3B and D, and moves the average and median volume across the protein closer together (i.e.,

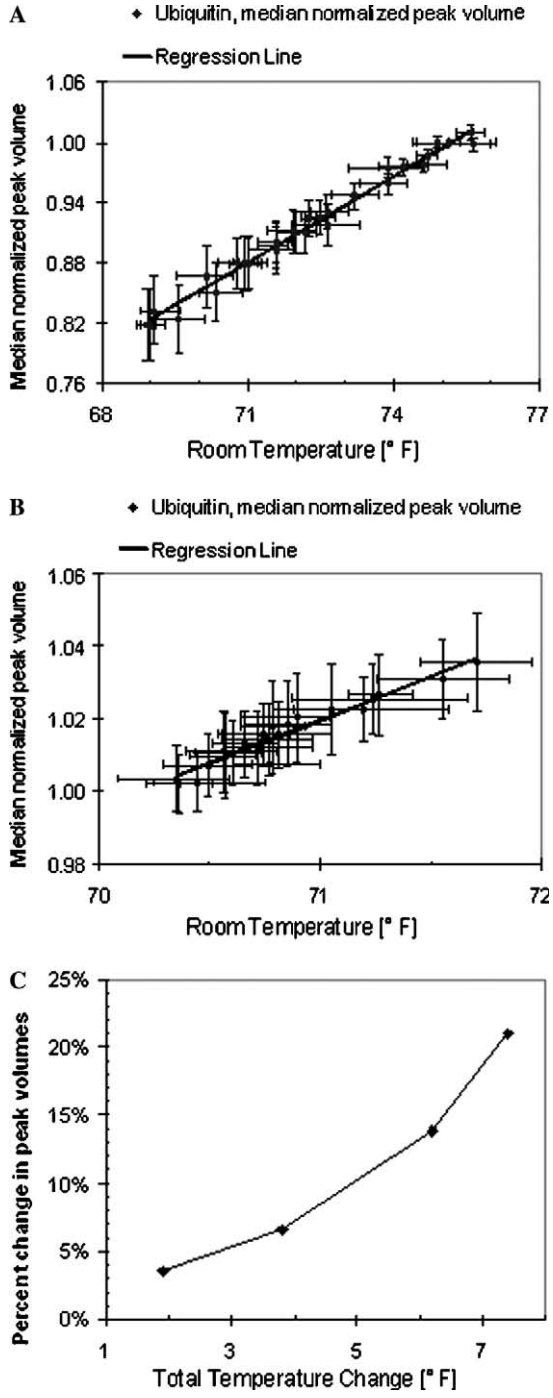

Fig. 2. Correlation between room temperature and peak volumes observed in ubiquitin control experiments (T_2[CPMG] experiment with a 4 ms relaxation delay), at constant sample temperature. (A) Observed volume changes when room temperature fluctuates between 68.7 and 76.1 °F. The correlation coefficient, r, is 0.99, and the significance of the correlation (probability that it is observed by chance) is $P(r) = 1.6 \times 10^{-27}$. (B) Observed volume changes when room temperature fluctuates between 69.6 and 71.5 °F (temperature controlled within ±1 °F). The value of $r = 0.97$, and $P(r) = 2.1 \times 10^{-13}$. (C) Percent change in observed volumes as a function of total change in room temperature.

outliers have been reduced). The standard deviation of volumes within a given experiment is also reduced, despite propagation of random error from the re-normalization values.

2.7. Mitigation of systematic error can significantly improve accuracy

The impact of mitigating the effects of systematic error can be observed by projecting the deviations observed in the original (measured) volumes (Fig. 3A) and the re-normalized volumes (Fig. 3B) onto a simulated relaxation dispersion curve, as shown in Fig. 4. While small contributions from random deviations and residual systematic error remain following re-normalization, their impact is significantly reduced. The parameters obtained from the fit to the curve in Fig. 4C are an order of magnitude more accurate than the parameters obtained from the fit to the curve in Fig. 4B, as shown in Table 1.

2.8. Choosing a control experiment for re-normalization

For successful re-normalization, a control experiment needs to reflect, as accurately as possible, the systematic effects that impact the data. Hence, as much as possible, the control experiments should have the same information content as the desired data. The most straightforward way to achieve this goal is to use the same basic experiment type for both measurement and control. For a relaxation series, one would wish to repeat the experiment that yields the highest intensities so that control information is available for all possible peaks. The desire for maximum information content must be balanced against the need to measure control experiments in a timely manner. As discussed in detail below, our experience shows that for systems with reasonable resolution and/or good signal-to-noise ratios, adequate information content can be retained while reducing the spectral resolution and/or the number of transients of the control measurements.

2.9. Choosing a protocol for re-normalization

The re-normalization protocol proposed above (re-normalizing an experimental peak using the average volume of the same peak observed in the immediately preceding and following control experiments) is clearly effective, as Fig. 3 illustrates. However, alternative protocols may provide advantages in specific situations. In particular, for some systems, control measurements performed with decreased spectral resolution or number of transients may result in information loss, i.e., overlapped or missing peaks. For these peaks, the protocol of re-normalization by individual control peak volume is inapplicable, and alternative protocols must be considered. A simple alternative is to substitute the average or median peak volume in each control experiment for the value of an individual control peak (see Section 4.5). This is a sensible alternative when the size of the systematic changes exceeds the standard deviation in peak volumes, as illustrated in Fig. 1C.

The results of re-normalization using average or median peak volumes are illustrated in Figs. 3C and D. While neither of these protocols performs as well as re-normalization

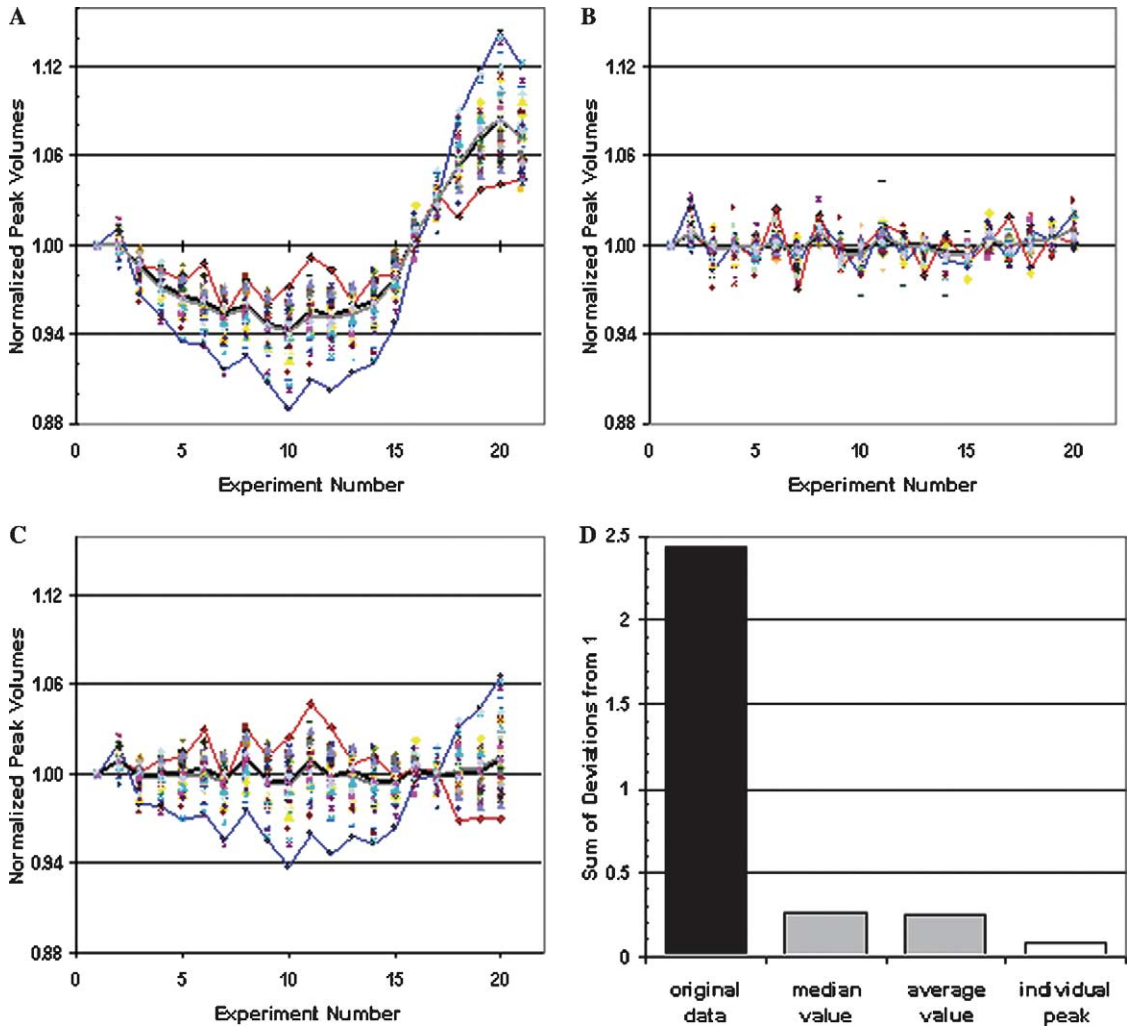

Fig. 3. Re-normalization of control experiments reproduces the expected distribution. (A) Observed volumes in a set of control measurements as a function of experiment number. (B) Volumes following re-normalization by individual peak volumes. (C) Volumes following re-normalization by average peak volume. (D) The sum of deviations from the constant value of 1 obtained in the original data and following re-normalization. (A–C) Each point indicates the volume of an individual ubiquitin peak. The envelope of observed peak volumes is outlined by tracing the peaks with the smallest (red line) and largest (blue line) fluctuations in the original data. The gray line indicates the average volume across the protein, while the black line indicates the median volume across the protein.

using individual peak volumes, both protocols substantially reduce the deviations observed in the original data. Re-normalization by the median volume is the method of choice if compromised data points (overlapped peaks or noise peaks) have not been carefully removed from the control set, while re-normalization by the average volume is the method of choice in the absence of compromised data points. In summary, all three protocols shown in Fig. 3 significantly reduce the deviation of peak volumes from the expected functional form; however, peak-specific changes are removed only by peak-specific re-normalization (Fig. 3B).

The success of these three protocols was also compared with the results of alternative methods, based on fitting the average volumes obtained in the control experiments to smooth functional forms. Each protocol was assessed as above and was found to provide inferior results (data not shown).

2.10. Systematic error can be reduced using control experiments: a practical example

To demonstrate the practical utility of the re-normalization protocol we must show that deviations from the expected functional form are also reduced for relaxation measurements, and that control measurements can be obtained in reasonable amounts of spectrometer time. A "standard" T_1 relaxation experiment was used for this demonstration. Experimental data were collected as described in Section 4.1. The data points along the T_1 relaxation decay were acquired with a measurement time of 10.3 h per spectrum, in "pseudo-random" order. To conserve spectrometer time, the control experiments were acquired with reduced resolution, for a measurement time of 2.3 h per spectrum.

Despite reduced resolution, the control experiments continue to perform well for both detecting and mitigating the

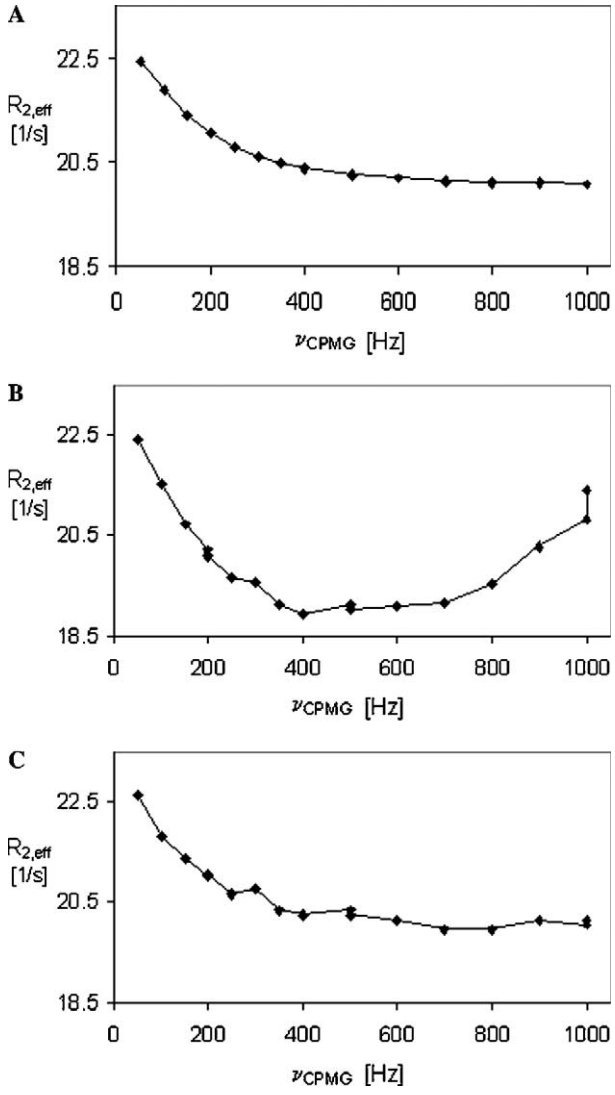

Fig. 4. Effect of systematic error on hypothetical relaxation dispersion curves at 500 MHz. (A) Error-free dispersion curve. (B) Dispersion curve with the addition of systematic error observed in the control experiments of Fig. 3A. (C) Dispersion curve with the addition of residual systematic error from the re-normalized control experiments of Fig. 3B. The parameters obtained from the fit to each curve are shown in Table 1.

impact of systematic error. The presence of systematic error is clearly revealed by the control experiments, as shown in Fig. 5A. The deviations from the expected functional form, induced by the systematic error, were reduced following re-normalization. This is illustrated by the improved reproducibility between replicate points, shown in Fig. 5C, and the improvement in the shape of the T_1 decay curve, shown in Fig. 5B. Re-normalization using alternative protocols resulted in inferior error correction (data not shown).

2.11. Control experiments provide significant benefits without excessive investment of spectrometer time

Since control experiments can be shortened without compromising their utility, they are very competitive with replicate measurements for spectrometer time, with potential for increased benefit. Duplicate or replicate measurements are often used to provide an estimate of the errors in relaxation data [30,31]. However, due to the small number of repeated data points, the error obtained from the replicate measurements is often judged "too small," and a minimum fixed value uncertainty, such as 2%, is substituted for the error from the repeat measurements [10,11]. The reported number of duplicate measurements commonly performed in a series of relaxation dispersion experiments varies from a minimum of two duplicate points, to a maximum of one duplicate at each point [11,23,31,32]. Using the same time ratio for experiment/control (~4:1) as used to obtain the results shown in Fig. 5, one could perform 8–26 control experiments in the time required for 2–6 duplicate measurements.

The control experiments provide substantial benefit both in the absence and in the presence of systematic error. In the absence of system-specific systematic error, the control experiments demonstrate that only experiment-specific errors and random errors need to be considered. The observed deviations in the controls also provide a comprehensive measure of the random error in the data. In the presence of system-specific systematic error, the control

Table 1
Effect of observed systematic error (Figs. 3A and B) on fast-exchange parameters in simulated relaxation dispersion experiments at 500 or 800 MHz

500 MHz	Parameters underlying error-free dispersion curve (Fig. 4A)	Parameters (and % err) from fit to dispersion curve in presence of observed err in Fig. 3A	Parameters (and % err) from fit to dispersion curve in presence of residual err in Fig. 3B
$\tau_{ex} = 1/k_{ex}$	9.34×10^{-4} s	20×10^{-4} s (120%)	10×10^{-4} s (11%)
$p_a \times p_b \times \delta\omega^2$	3.18×10^3 s^{-2}	2.4×10^3 s^{-2} (24%)	3.1×10^3 s^{-2} (2.5%)
$R_2(\nu_{CPMG} = \infty)$	20.0 s^{-1}	19.6 s^{-1} (2%)	20.0 s^{-1} (0.002%)
800 MHz	Parameters underlying error-free dispersion curve	Parameters (and % err) from fit to dispersion curve in presence of observed err in Fig. 3A	Parameters (and % err) from fit to dispersion curve in presence of residual err in Fig. 3B
$\tau_{ex} = 1/k_{ex}$	9.34×10^{-4} s	14.0×10^{-4} s (49%)	9.73×10^{-4} s (4%)
$p_a \times p_b \times \delta\omega^2$	8.14×10^3 s^{-2}	6.64×10^3 s^{-2} (18%)	8.08×10^3 s^{-2} (0.8%)
$R_2(\nu_{CPMG} = \infty)$	25.25 s^{-1}	24.98 s^{-1} (1%)	25.25 s^{-1} (0.0004%)

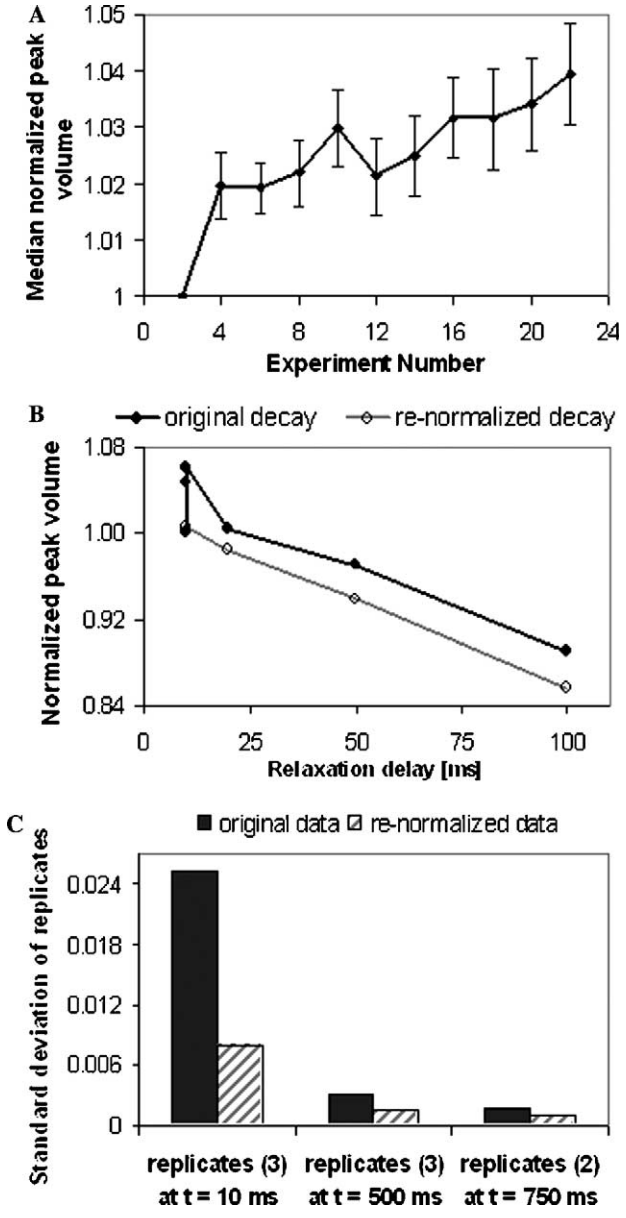

Fig. 5. Re-normalization of measured points along an exponential decay using control experiments. (A) Systematic changes in peak volumes observed in control experiments during a series of T_1 relaxation measurements. Error bars represent the standard deviation of non-overlapped peak volumes across the protein. (B) The shape of the T_1 decay curve before and after re-normalization. (C) The standard deviation between replicate points before and after re-normalization.

experiments report on the magnitude of the systematic changes, provide a means for reducing the systematic error by re-normalization, and provide an upper bound on the random error.

3. Conclusions

New measurements require new treatments of systematic error. Relaxation dispersion curves can be difficult to characterize at low spectrometer frequencies (500–600 MHz), due to shallow curvature and large experimental error. Simply collecting data at higher field strengths does not solve the problem, since proper interpretation of data requires that dispersion curves be characterized at multiple field strengths. Where possible, sources of experimental error must be identified and reduced or removed. We have shown that system-specific systematic error can be identified and quantified using control experiments. Quantifying the extent of systematic error is important for reliable data interpretation and useful for social engineering, such as justification for system upgrades (vibration isolation, environmental controls, etc.).

In the absence of systematic error, control experiments provide a comprehensive measure of random error. When systematic error is present, and the systematic changes are correlated and continuous, control experiments can be used to re-normalize experimental data, reducing the impact of the systematic error on relaxation measurements. In this case, the controls serve as an upper bound on the random error. Control experiments need not be full-length replicates; rather, they can be run with reduced resolution or reduced number of transients to make optimal use of spectrometer time. Based on these observations, we conclude that replacing a small set of replicates with a complete set of controls is likely to be beneficial for analysis of relaxation dispersion measurements at any magnetic field strength, and critical for successful analysis at lower field strengths.

4. Experimental

4.1. NMR spectroscopy

Relaxation measurements were performed on either a 1.2 or a 2.3 mM [U-^{15}N] sample of ubiquitin (90% H_2O/10% D_2O, 50 mM potassium phosphate buffer, pH 5.8). Relaxation data were collected on a Bruker AVANCE 500 MHz spectrometer, using a 5 mm self-shielded triple-resonance probe with triple-axis gradients. Measurement temperatures were set to 298 or 278 K as reported by the instrument control panel. Independent calibration with a methanol standard demonstrated that measurements reported at 298 K corresponded to an actual temperature of 297.7–297.8 K.

Backbone ^{15}N T_1 and T_2 (CPMG) values were measured using published procedures [33]. The interpulse delay between ^{15}N 180° pulses in the CPMG sequence was 1.0 ms. All 2D experiments were measured with a recycle delay of 2.5 s [17], and a spectral width of 1.8×5.0 kHz in the $t1 \times t2$ dimensions. The control experiments shown in Figs. 1–3 were measured using the T_2 (CPMG) experiment with a 4 ms relaxation delay, 16 transients per $t1$ increment (using the 2.3 mM sample), and 50×1024 complex points in the $t1 \times t2$ dimensions, resulting in a measurement time of 1.28 h per spectrum. The T_1 relaxation measurements and control experiments shown in Fig. 5 were acquired with 32 transients per $t1$ increment (using the 1 mM sample), and 200×1024 complex points or 45×1024 complex points in the $t1 \times t2$ dimensions, result-

ing in measurement times of 10.3 or 2.3 h per spectrum, respectively. Points were collected along the T_1 relaxation decay in "pseudo-random" order (10, 20, 750, 50, 500, 100, 10, 750, 500, 10, and 500 ms). T_1 control experiments were measured with a 10 ms relaxation delay.

4.2. Alternative control experiments

Lock levels were measured and written to a text file between each experiment using a modification of the Bruker automation program *multizg* and the Bruker function *mygetlock*. The modified automation program is available from the authors upon request.

Measurements of the water signal intensity were performed using a simple one-pulse experiment [34], with a recycle delay of 1.77 s, a spectral width of 1.4 kHz, 8 transients per experiment and 1024 complex points, for a total measurement time of 25 s. The spectra were zero-filled, Fourier-transformed and phased using NMRPipe and the intensity of the water peak was extracted using nmrDraw [35].

1D Watergate experiments [36] were performed using a rectangular 2 ms water flip-back pulse, *z*-gradients of 30 G/cm, a recycle delay of 1.84 s, a spectral width of 7002 Hz, 16 transients per experiment and 8192 complex points, for a total measurement time of 2 m 31 s. Spectra were processed and integrated using Bruker XWINNMR 2.6 software.

4.3. Data Processing

All 2D NMR spectra were processed using the NMRPipe and nmrDraw software tools [35]. For short 2D control experiments (50 or fewer complex points in the $t1$ dimension) the $t1$ interferogram was extended by linear prediction. For data collected at 298 K, the cosine bell window function was applied to the $t1$ interferograms, while Lorentzian-to-Gaussian transformations with exponential linewidths of 15 Hz and Gaussian linewidths of 22 Hz were applied to the $t2$ interferograms. For data collected at 278 K, cosine bell window functions were applied to both the $t1$ and $t2$ interferograms. Peak volumes were obtained using nonlinear least squares analysis of peak line-shapes as implemented in nlinLS [35], and normalized using the SCALE1D function.

4.4. Assessing random vs. systematic effects

To assess the probability that observed deviations in control experiments are attributable to random error alone, or whether systematic error is likely to be present, the following expression was implemented: $\chi^2 = \sum_{i=1}^{n}(\frac{\bar{O}_i - E_i}{\sigma_i})^2$ where $\bar{\boldsymbol{O}}_{\boldsymbol{i}}$ is the observed median or average volume for the control experiment i (median if overlapped and noise peaks are present, average if they are removed), $\boldsymbol{E}_{\boldsymbol{i}}$ is the expected value for the control experiment in the absence of error (i.e., 1), and $\sigma_{\boldsymbol{i}}$ is the standard deviation of volumes across the control experiment. The one-tailed probability of the chi-squared distribution was used to assess the hypothesis that the deviations from the expected value are observed by chance. Small probabilities indicate that the discrepancies are unlikely to be chance fluctuations, and the measurement errors may not be normally distributed [37].

4.5. Re-normalization of experimental data

Re-normalization of experimental data using individual control peak volumes was performed according to the following expression:

$$\boldsymbol{P}_{\boldsymbol{i,RN}} = \frac{\boldsymbol{P}_{\boldsymbol{i}}}{(\boldsymbol{C}_{\boldsymbol{i,n-1}} + \boldsymbol{C}_{\boldsymbol{i,n+1}})/2},$$

where $P_{i,RN}$ is the re-normalized volume of peak i, P_i is the measured volume of peak i, $C_{i,n-1}$ and $C_{i,n+1}$ are the volumes of the same peak in the control measurements immediately preceding and following experiment n.

Re-normalization based on the net characteristics of control experiments (such as average or median peak volume across the protein) was performed according to the alternative expression:

$$\boldsymbol{P}_{\boldsymbol{i,RN}} = \frac{\boldsymbol{P}_{\boldsymbol{i}}}{(\bar{\boldsymbol{C}}_{\boldsymbol{n-1}} + \bar{\boldsymbol{C}}_{\boldsymbol{n+1}})/2},$$

where $P_{i,RN}$ is the re-normalized volume of peak i, P_i is the measured volume of peak i, and $\bar{\boldsymbol{C}}$ represents the average or median peak volume in the immediately preceding and following control experiments. As noted in Section 2, when re-normalizing based on net characteristics, use of the median volume is recommended if compromised data points (overlapped peaks or noise peaks) have not been carefully removed, while use of the average volume is recommended in the absence of compromised data points. In general, re-normalization based on net characteristics of a control experiment is only preferable to re-normalization based on individual control peak volumes for cases in which compromised control peaks prevent peak-specific correction.

4.6. Simulated exponential decay curves

Exponential decay curves were constructed from the function $\boldsymbol{I}(\boldsymbol{t}) = \boldsymbol{e}^{-R_2 t}$, where R_2 was set to 20 s^{-1}. Values were calculated at 6 time points (4, 10, 20, 50, 100, and 150 ms) with repeat points at 4 (3×), 100 (3×), and 150 (2×) ms, for a total of 11 points. Random errors, drawn from a uniform distribution of mean zero and standard deviation $0.014I$, were added to each value in the decay curve [now referred to as $I^*(t)$]. Systematic errors of up to 5% were drawn from two types of underlying error (systematic increase or systematic decrease in intensity), and four possible collection orders (increasing increment, decreasing increment, alternating large and small increments [triangular], and "pseudo-random," Supplemental Fig. S1). Systematic errors were added to the values of

$I^*(t)$ to generate final values, $I^{**}(t)$. These values were fit to exponential decay curves under the deliberately naïve assumption that the data were impacted only by 2.5% random error. Decay curves were fit using the Levenberg–Marquardt algorithm, as implemented in PrestoPlot (www.mbg.cornell.edu/Shalloway_Lab_Presto.cfm). The values of the percent error in parameters obtained from these fits are reported in Section 1 and in Table S1.

4.7. Simulated relaxation dispersion curves

Relaxation dispersion curves were generated from the equation for fast exchange between two states:

$$R_2(\nu_{\mathrm{CPMG}}) = R_2(\nu_{\mathrm{CPMG}} = \infty) + (p_a p_b \delta\omega^2/k_{ex}) \times (1 - [4\nu_{\mathrm{CPMG}}/k_{ex}] * \tanh[k_{ex}/4\nu_{\mathrm{CPMG}}]),$$

where ν_{CPMG} is $1/(4\tau)$, and 2τ is the time between centers of successive 180° pulses, p_b is the population in state b, $p_a = 1 - p_b$, $\delta\omega$ is the difference in chemical shift between the two states, and k_{ex} is the sum of the exchange rates from state a to state b, and state b to state a. The parameters of the function were set to the values shown in Table 1.

To obtain the error values cited in Section 1, the values cited in Table S1, and the simulated dispersion curves of Figs. 1A and B, values of $R_2(\nu_{\mathrm{CPMG}})$ were calculated at 12 frequency points (50, 100, 150, 200, 300, 400, 500, 600, 700, 800, 900, and 1000 Hz) with repeat points at 200, 500, and 1000 Hz, for a total of 15 points. Random errors, drawn from a uniform distribution of mean zero and standard deviation 0.014 R, were added to each value in the decay curve [now referred to as $R_2^*(\nu_{\mathrm{CPMG}})$]. Systematic errors of up to 5% in intensity were propagated to obtain systematic errors in $R_2(\nu_{\mathrm{CPMG}})$ of up to 5.9% at 500 MHz ($\frac{\Delta R_2}{R_2} = -|\frac{\Delta I}{I}|/\ln[\frac{I}{I_0}], \ln[\frac{I}{I_0}] \sim 0.85$), and 4.4% at 800 MHz ($\ln[\frac{I}{I_0}] \sim 1.1$). The systematic errors in the relaxation dispersion curves were generated to represent the same underlying errors and data collection orders (Supplemental Fig. S2) as were examined for the exponential decay curves. Systematic errors were added to the values of $R_2^*(\nu_{\mathrm{CPMG}})$ to generate final values, $R_2^{**}(\nu_{\mathrm{CPMG}})$. These values were fit to the two-site fast-exchange equation under the deliberately naïve assumption that the data were impacted only by 2.5% random error. Decay curves were fit with PrestoPlot, as described above.

To obtain the values shown in Table 1 and the simulated dispersion curves shown in Fig. 4, values of $R_2(\nu_{\mathrm{CPMG}})$ were calculated at 14 frequency points (50, 100, 150, 200, 250, 300, 350, 400, 500, 600, 700, 800, 900, and 1000 Hz) with repeat points at 200, 500, and 1000 Hz, for a total of 17 points. Errors observed in the control experiments of Figs. 3A and B, were propagated to obtain errors in $R_2(\nu_{\mathrm{CPMG}})$, assuming that points along the dispersion curve were collected in order of increasing ν_{CPMG}. The errors were added to the values of $R_2(\nu_{\mathrm{CPMG}})$ to obtain final values that were fit to the two-site fast-exchange equation using PrestoPlot.

4.8. Temperature measurements

Changes in room temperature were observed with a National Semiconductor precision Fahrenheit temperature sensor (LM34), positioned approximately one foot from the outside of the spectrometer, and vertically centered on the magnetic field coils. The temperature sensor was interfaced with a desktop computer through a PCI-DAS4020/12 ADC board (Measurement Computing). The data were converted to read-out temperature using the SoftWIRE graphical programming interface. A measurement was recorded every 30 s and stored to the hard drive along with the time and date stamp for later analysis. Additional discussion of the effects of room temperature changes on peak volumes is offered in the Supplemental Information.

Sample temperature measurements were performed using a methanol standard (4% CH_3OH in CD_3OD) to verify that observed changes in intensity were not a function of changing sample temperature. Each 1D methanol spectrum was collected using four transients and four dummy scans, with 4096 complex points. The recycle delay was set to 31.5 s, resulting in a measurement time of 4.4 min per spectrum. To approximate the sample conditions in relaxation measurements as closely as possible, a mock T_2 (CPMG) experiment was run between each 1D methanol spectrum. Measurements were performed over a total period of 16.5 h. Over the collection period, the sample temperature changed by ~0.1 K (Supplemental Fig. S3a). Since relaxation rates are expected to change by ~3% per K [23], the observed change in sample temperature does not explain the observed changes in intensity. Further, the changes in methanol sample temperature were *uncorrelated* with the changes in room temperature, with a correlation coefficient, r, of 0.43, and a significance value (probability of being observed by chance) greater than 0.15 (15%) (Supplemental Fig. S3b). Over the same period, the changes in methanol peak intensities were strongly correlated with changes in room temperature, with a correlation coefficient of 0.99, and a significance value of 4.5×10^{-10} (Supplemental Fig. S3c).

Acknowledgments

We thank Jason D. Gans (LANL), Amy Freund (Bruker Biospin) and Martine Monette (Bruker Biospin) for valuable comments and discussion. For spectrometer time, we thank the High Field Magnetic Resonance Facility at the Environmental Molecular Sciences Laboratory, a national scientific user facility sponsored by the Department of Energy's Office of Biological and Environmental Research and located at Pacific Northwest National Laboratory. N. H. Pawley was supported by NIH Grant F32GM071263. Additional support for this work was provided by the Los Alamos National Laboratory LDRD program, Grant X1VE, and NIH Grant EB002166.

Appendix A. Supplementary data

Supplementary data associated with this article can be found, in the online version, at doi:10.1016/j.jmr.2005.08.017.

References

[1] H.J. Dyson, P.E. Wright, Unfolded proteins and protein folding studied by NMR, Chem. Rev. 104 (2004) 3607–3622.

[2] M. Akke, NMR methods for characterizing microsecond to millisecond dynamics in recognition and catalysis, Curr. Opin. Struct. Biol. 12 (2002) 642–647.

[3] A.J. Wand, S.W. Englander, Protein complexes studied by NMR spectroscopy, Curr. Opin. Biotechnol. 7 (1996) 403–408.

[4] M.J. Stone, NMR relaxation studies of the role of conformational entropy in protein stability and ligand binding, Acc. Chem. Res. 34 (2001) 379–388.

[5] A.M. Mandel, M. Akke, A.G. Palmer, Dynamics of ribonuclease H: temperature dependence of motions on multiple time scales, Biochemistry 35 (1996) 16009–16023.

[6] L.E. Kay, Protein dynamics from NMR, Biochem. Cell Biol. 76 (1998) 145–152.

[7] J.A. Jones, P. Hodgkinson, A.L. Barker, P.J. Hore, Optimal sampling strategies for the measurement of spin–spin relaxation times, J. Magn. Reson. B 113 (1996) 25–34.

[8] N.J. Skelton, A.G. Palmer III, M. Akke, J. Kordel, M. Rance, W.J. Chazin, Practical aspects of two-dimensional proton-detected {sup 15}N spin relaxation measurements, J. Magn. Reson. B 102 (1993) 253–264.

[9] C. Bracken, P.A. Carr, J. Cavanagh, A.G. Palmer, Temperature dependence of intramolecular dynamics of the basic leucine zipper of GCN4: implications for the entropy of association with DNA, J. Mol. Biol. 285 (1999) 2133–2146.

[10] D.M. Korzhnev, E.V. Bocharov, A.V. Zhuravlyova, V.Y. Orekhov, T.V. Ovchinnikova, M. Billeter, A.S. Arseniev, Backbone dynamics of the channel-forming antibiotic zervamicin IIB studied by 15N NMR relaxation, FEBS Lett. 495 (2001) 52–55.

[11] A.A. Di Nardo, D.M. Korzhnev, P.J. Stogios, A. Zarrine-Afsar, L.E. Kay, A.R. Davidson, Dramatic acceleration of protein folding by stabilization of a nonnative backbone conformation, Proc. Natl. Acad. Sci. USA 101 (2004) 7954–7959.

[12] A.G. Palmer, N.J. Skelton, W.J. Chazin, P.E. Wright, M. Rance, Suppression of the effects of cross-correlation between dipolar and anisotropic chemical shift relaxation mechanisms in the measurement of spin–spin relaxation rates, Mol. Phys. 75 (1992) 699–711.

[13] M. Czisch, G.C. King, A. Ross, Removal of systematic errors associated with off-resonance oscillations in T{sub 2} measurements, J. Magn. Reson. 126 (1997) 154–157.

[14] A. Ross, M. Czisch, G.C. King, Systematic errors associated with the CPMG pulse sequence and their effect on motional analysis of biomolecules, J. Magn. Reson. 124 (1997) 355–365.

[15] G.N. Yip, E.R. Zuiderweg, A phase cycle scheme that significantly suppresses offset-dependent artifacts in the R{sub 2}-CPMG {sup 15}N relaxation experiment, J. Magn. Reson. 171 (2004) 25–36.

[16] D.M. Korzhnev, E.V. Tischenko, A.S. Arseniev, Off-resonance effects in 15N T2 CPMG measurements, J. Biomol. NMR 17 (2000) 231–237.

[17] S.M. Gagne, S. Tsuda, L. Spyracopoulos, L.E. Kay, B.D. Sykes, Backbone and methyl dynamics of the regulatory domain of troponin C: anisotropic rotational diffusion and contribution of conformational entropy to calcium affinity, J. Mol. Biol. 278 (1998) 667–686.

[18] D.M. Korzhnev, N.R. Skrynnikov, O. Millet, D.A. Torchia, L.E. Kay, An NMR experiment for the accurate measurement of heteronuclear spin-lock relaxation rates, J. Am. Chem. Soc. 124 (2002) 10743–10753.

[19] A. Allerhand, H.S. Gutowsky, Spin-echo NMR studies of chemical exchange.1. Some general aspects, J. Chem. Phys. 41 (1964) 2115.

[20] J.H. Viles, B.M. Duggan, E. Zaborowski, S. Schwarzinger, J.J.A. Huntley, G.J.A. Kroon, H.J. Dyson, P.E. Wright, Potential bias in NMR relaxation data introduced by peak intensity analysis and curve fitting methods, J. Biomol. NMR 21 (2001) 1–9.

[21] C.Y. Wang, N.H. Pawley, L.K. Nicholson, The role of backbone motions in ligand binding to the c-Src SH3 domain, J. Mol. Biol. 313 (2001) 873–887.

[22] L. Vugmeyster, O. Trott, C.J. McKnight, D.P. Raleigh, A.G. Palmer, Temperature-dependent dynamics of the villin headpiece helical subdomain, an unusually small thermostable protein, J. Mol. Biol. 320 (2002) 841–854.

[23] V.Y. Orekhov, D.M. Korzhnev, T. Diercks, H. Kessler, A.S. Arseniev, H-1-N-15 NMR dynamic study of an isolated alpha-helical peptide (1–36)-bacteriorhodopsin reveals the equilibrium helix–coil transitions, J. Biomol. NMR 14 (1999) 345–356.

[24] O. Millet, J.P. Loria, C.D. Kroenke, M. Pons, A.G. Palmer, The static magnetic field dependence of chemical exchange linebroadening defines the NMR chemical shift time scale, J. Am. Chem. Soc. 122 (2000) 2867–2877.

[25] J.G. Kempf, J.P. Loria, Protein dynamics from solution NMR: theory and applications, Cell Biochem. Biophys. 37 (2003) 187–211.

[26] N.R. Skrynnikov, F.W. Dahlquist, L.E. Kay, Reconstructing NMR spectra of ''invisible'' excited protein states using HSQC and HMQC experiments, J. Am. Chem. Soc. 124 (2002) 12352–12360.

[27] F.A.A. Mulder, N.R. Skrynnikov, B. Hon, F.W. Dahlquist, L.E. Kay, Measurement of slow (mu s-ms) time scale dynamics in protein side chains by N-15 relaxation dispersion NMR spectroscopy: application to Asn and Gln residues in a cavity mutant of T4 lysozyme, J. Am. Chem. Soc. 123 (2001) 967–975.

[28] A.G. Palmer, C.D. Kroenke, J.P. Loria, Nuclear magnetic resonance methods for quantifying microsecond-to-millisecond motions in biological macromolecules, in: T.L. James, V. Doetsch, U. Schmitz (Eds.), Nuclear Magnetic Resonance of Biological Macromolecules Part B, Academic Press, San Diego, 2001, pp. 204–238.

[29] R.L. McFeeters, R.E. Oswald, Structural mobility of the extracellular ligand-binding core of an ionotropic glutamate receptor. Analysis of NMR relaxation dynamics, Biochemistry 41 (2002) 10472–10481.

[30] R.B. Hill, C. Bracken, W.F. DeGrado, A.G. Palmer, Molecular motions and protein folding: characterization of the backbone dynamics and folding equilibrium of alpha D-2 using C-13 NMR spin relaxation, J. Am. Chem. Soc. 122 (2000) 11610–11619.

[31] F.A.A. Mulder, B. Hon, A. Mittermaier, F.W. Dahlquist, L.E. Kay, Slow internal dynamics in proteins: application of NMR relaxation dispersion spectroscopy to methyl groups in a cavity mutant of T4 lysozyme, J. Am. Chem. Soc. 124 (2002) 1443–1451.

[32] A. Mittermaier, L.E. Kay, The response of internal dynamics to hydrophobic core mutations in the SH3 domain from the Fyn tyrosine kinase, Protein Sci. 13 (2004) 1088–1099.

[33] N.A. Farrow, O.W. Zhang, J.D. Forman-Kay, L.E. Kay, A heteronuclear correlation experiment for simultaneous determination of N-15 longitudinal decay and chemical-exchange rates of systems in slow equilibrium, J. Biomol. NMR 4 (1994) 727–734.

[34] J. Cavanagh, W.J. Fairbrother, A.G. Palmer III, N.J. Skelton, in: Protein NMR spectroscopy: Principles and practice, Academic Press, San Diego, 1996, pp. 95–182.

[35] F. Delaglio, S. Grzesiek, G.W. Vuister, G. Zhu, J. Pfeifer, A. Bax, NMRPipe: a multidimensional spectral processing system based on UNIX pipes, J. Biomol. NMR 6 (1995) 277–293.

[36] M. Piotto, V. Saudek, V. Sklenar, Gradient-tailored excitation for single-quantum NMR spectroscopy of aqueous solutions, J. Biomol. NMR 2 (1992) 661–665.

[37] W.H. Press, S.A. Teukolsky, W.T. Vetterling, B.P. Flannery, in: Numerical Recipes in C: The Art of Scientific Computing, Cambridge University Press, New York, 1992, pp. 656–706.